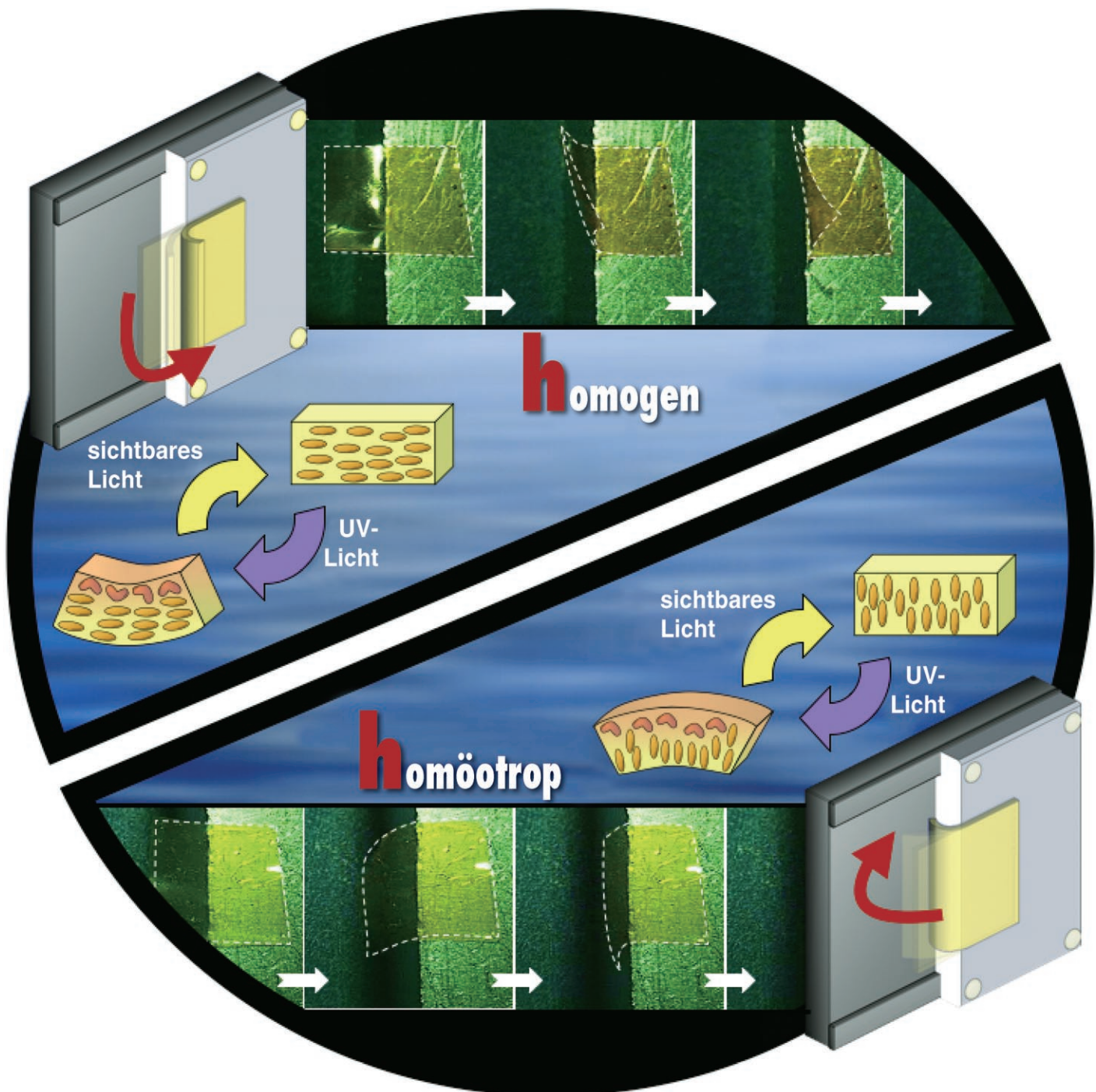


Zuschriften



Flüssigkristalline Azobenzolelastomerfilme mit zwei Arten der Mesogenausrichtung, parallel (homogen) und senkrecht (homöotrop) zur Filmoberfläche, wurden durch Photopolymerisation erhalten. T. Ikeda et al. diskutieren in ihrer Zuschrift auf den folgenden Seiten, wie die Ausrichtung der Mesogene das Biegeverhalten der Filme bei Bestrahlung mit UV/Vis-Licht bestimmt.

How Does the Initial Alignment of Mesogens Affect the Photoinduced Bending Behavior of Liquid-Crystalline Elastomers?

Mizuho Kondo, Yanlei Yu, and Tomiki Ikeda*

The development of actuators that show bending movement is of increasing interest. The bending movement is usually induced by an asymmetric contraction or expansion in the materials.^[1–4] This type of actuator has more advantages than the actuators that show only two-dimensional movements, such as expansion and contraction, from the viewpoint of precise three-dimensional actuation and long lifetime owing to small deformation for the bending action. Because of these unique properties, the bending actuators are expected to be used for cantilevers, micropumps, and many other micro-mechanical applications.

Various materials have been reported as the bending actuators, such as piezoelectric transducers,^[5] shape-memory alloys,^[6] and polymers.^[2] In comparison with other materials, the polymer actuators are much softer, lighter, and highly processible, which makes them easily made into various shapes; consequently, studies have been performed on the actuation of polymer materials and many applications have been proposed.^[7] In addition, the bending of most polymer actuators, such as conducting polymers is driven by electrical energy; thus, these materials require wires to acquire electrical power.^[3] On the other hand, elastomeric polymers, including gels and shape-memory polymers, can undergo mechanical actuation in response to various physical stimuli, such as pH,^[8] solvent composition,^[9] heat,^[10–12] and light.^[13,14]

Light can be controlled remotely and rapidly as an external stimulus, so it is of great importance in developing simple, efficient, and compact elastomeric polymer actuators that can be driven by light. It is known that liquid-crystalline elastomers (LCEs) exhibit a spontaneous contraction along the director axis when heated above their nematic (N)–isotropic (I) phase-transition temperatures.^[15–17] On the other hand, when azobenzene chromophores are incorporated into LCEs, they can undergo the contraction isothermally because of the change in alignment order by light.^[18–20] Furthermore, as the extinction coefficient of the azobenzene moieties at

approximately 360 nm is large (about $2.0 \times 10^4 \text{ L mol}^{-1} \text{ cm}^{-1}$) and more than 99% of the incident photons are absorbed by the surface with a thickness of less than 1 μm , LCE films with a high concentration of azobenzene moieties can generate an alignment change only in the film surface upon exposure to actinic UV light. As a result, an uneven distribution of the anisotropic deformation is formed along the film normal and the bending action can be realized in the film. Previously, we found that monodomain and polydomain LCE films showed different bending behavior: the bending of the former took place just along the alignment direction of the mesogens,^[21] while in the latter the bending in any direction could be evoked.^[22] These results indicate that the initial alignment of photoactive mesogens strongly affects the bending behavior of the LCE films. In this study, therefore, we explored the effect of the initial alignment of the azobenzene mesogens on the bending behavior of the LCE films. For this purpose, we prepared LCE films with two extreme alignment modes, parallel (homogeneous) and normal (homeotropic) to the film surface, and investigated their photoresponsive behavior in detail.

The structures of the monofunctional LC monomer 6-4-(4-hexyloxyphenylazo)phenoxyhexyl acrylate (A6AB6) and difunctional monomer 4,4'-bis[6-(acryloyloxy)hexyloxy]azobenzene (DA6AB) used in this study are shown in Figure 1 a.

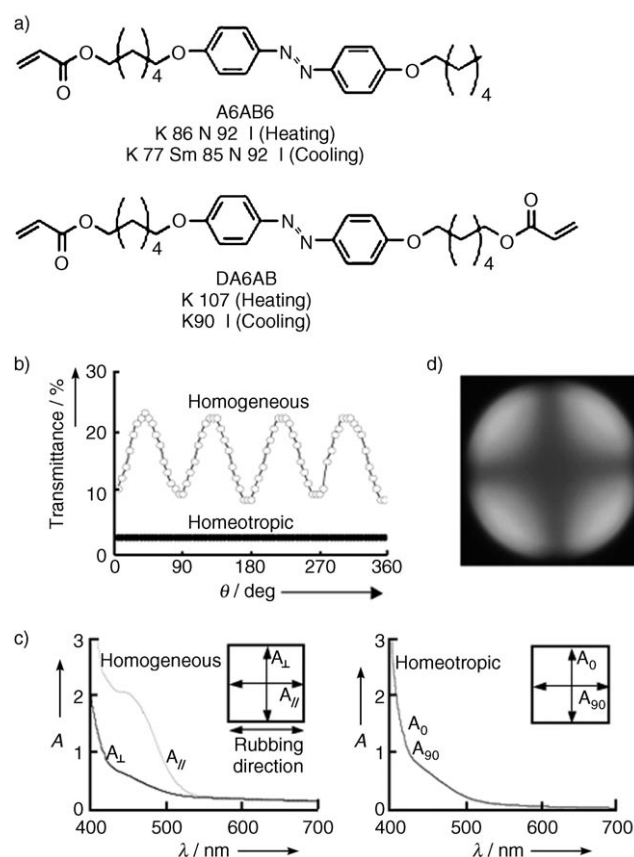


Figure 1. Structures of the LC monomer and cross-linker used in this study (a), and optical properties of the homogeneous and homeotropic films analyzed by POM (b), polarized UV/Vis absorption spectroscopy (c), and conoscopic observation by POM (d). Thickness of the films: 10 μm .

[*] M. Kondo, Prof. Dr. T. Ikeda
 Chemical Resources Laboratory
 Tokyo Institute of Technology, R1–11
 4259 Nagatsuta, Midori-ku, Yokohama 226-8503 (Japan)
 Fax: (+81) 45-924-5275
 E-mail: tikeda@res.titech.ac.jp
 Prof. Dr. Y. Yu
 Department of Materials Science
 Fudan University, 220 Handan Road
 Shanghai 200433 (China)

Supporting information for this article is available on the WWW under <http://www.angewandte.org> or from the author.

The mesomorphic properties of the monomers were studied by polarized-light optical microscopy (POM) and differential scanning calorimetry (DSC; see the Experimental Section). The typical schlieren texture of an N phase was observed at 86 °C for A6AB6, and isotropization occurred at 92 °C upon heating. When cooled from the I phase, the N phase appeared at 92 °C and a monotropic smectic (Sm) phase at 85 °C. Crystallization started at 77 °C. However, DA6AB did not show any mesomorphism.

It was found by DSC studies that the glass-transition temperature (T_g) of the LCE films appeared at approximately 60 °C, and the DSC curve also exhibited a broad endothermic peak at approximately 147 °C, which was assigned to the LC–I phase transition. The optical anisotropy in the LCE films was evaluated at room temperature by measuring the transmittance of the probe light through crossed polarizers with a sample film between them as a function of the rotation angle (Figure 1b). For the homogeneous films, the rotation angle indicates the direction of the polarizer with respect to the rubbing direction of the alignment layers. The regular maximum and minimum values with 90° separations show that the azobenzene mesogens in the homogeneous films are preferentially aligned along the rubbing direction of the alignment layers. On the other hand, the transmittance was quite low (<3%) in the homeotropic films and showed no angular dependence.

We also investigated the alignment behavior of the azobenzene mesogens by polarized absorption spectroscopy (Figure 1c). In the homogeneous films, A_{\parallel} and A_{\perp} are the absorbance measured with light polarized parallel and perpendicular to the rubbing direction of the alignment layers, respectively. In the homeotropic films, the polarization directions of the measurement beam for A_0 and A_{90} were perpendicular to each other. It is clear that the homogeneous films show high dichroism along the alignment direction, whereas the homeotropic films exhibit low absorption and no dichroism. In addition, the conoscopic observation of the homeotropic films by POM showed a dark cross image (Figure 1d). The cross point represents the optic axis of the LC phase; therefore, it is clear that the azobenzene mesogens are aligned normal to the film surface in the homeotropic films.

We observed the photoinduced-bending behavior of the LCE films under the experimental setup shown in Figure 2a. A part of a free-standing LCE film was pasted onto an aluminum block, heated by a hot stage, and irradiated with unpolarized UV light. We set the film vertically to eliminate the influence of gravity. When the homogeneous film was exposed to UV light at 366 nm, the film bent toward the irradiation direction of the actinic light along the alignment direction (see Figure 2b and the Supporting Information). On the other hand, when the homeotropic film was exposed to the actinic light, it bent away from the actinic light source (see Figure 2c and the Supporting Information). We observed completely different bending behavior in the LCE films with different alignment of azobenzene mesogens. Additionally, both the homogeneous and homeotropic films reverted to the initial flat states when irradiated with visible light at > 540 nm.

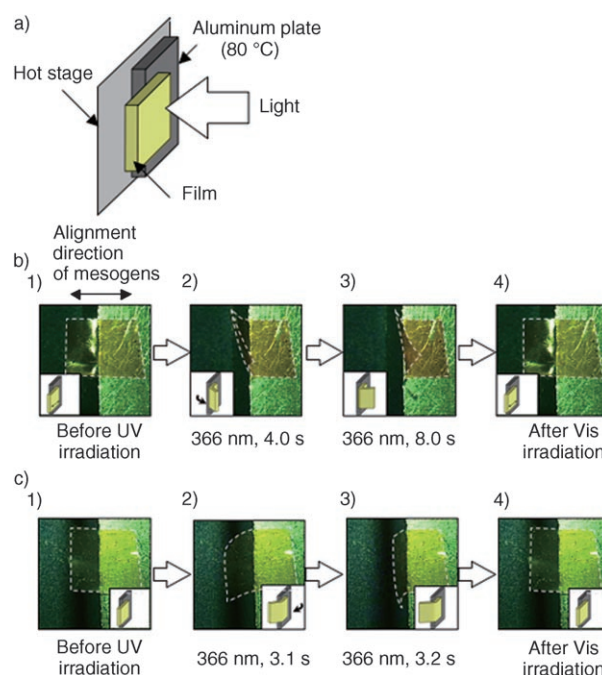


Figure 2. Schematic illustration of the experimental setup (a) and photographs of the homogeneous film (b) and the homeotropic film (c) that exhibits photoinduced bending and unbending behavior. The white dash lines show the edges of the films and the inset of each photograph is a schematic illustration of the film state. The intensity of 366 nm light was 50 mWcm^{-2} . Size of the films: $4 \text{ mm} \times 4 \text{ mm} \times 20 \mu\text{m}$. Vis = visible.

To observe the bending behavior of the homeotropic film in a more free-standing state, we set the film on a copper stick fixed to a copper plate, with which the temperature of the film was controlled (Figure 3a). When the film was irradiated with

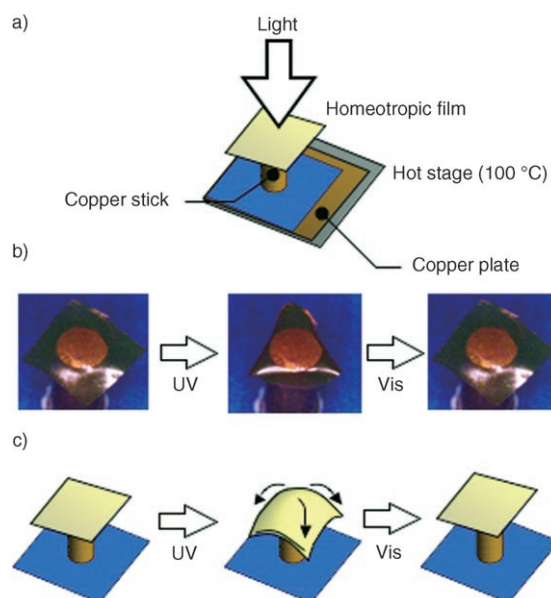


Figure 3. Schematic illustration of the experimental setup (a), photographs of the bending behavior of the homeotropic film (b), and schematic illustration of the film state (c). The intensity of 366 nm light was 35 mWcm^{-2} . Size of the film: $5 \text{ mm} \times 5 \text{ mm} \times 20 \mu\text{m}$.

366 nm light, all sides of the film bent away from the actinic light source simultaneously until they wrapped around the top of the copper stick (Figure 3b). This behavior indicates that the bending of the homeotropic film occurs isotropically without a preferential direction (Figure 3c), in a completely opposite way from the homogeneous film whose bending takes place anisotropically only along the alignment direction of mesogens.

A plausible mechanism of the bending behavior of the homogeneous and homeotropic films is illustrated in Figure 4a. It has been known that the irradiation of UV light

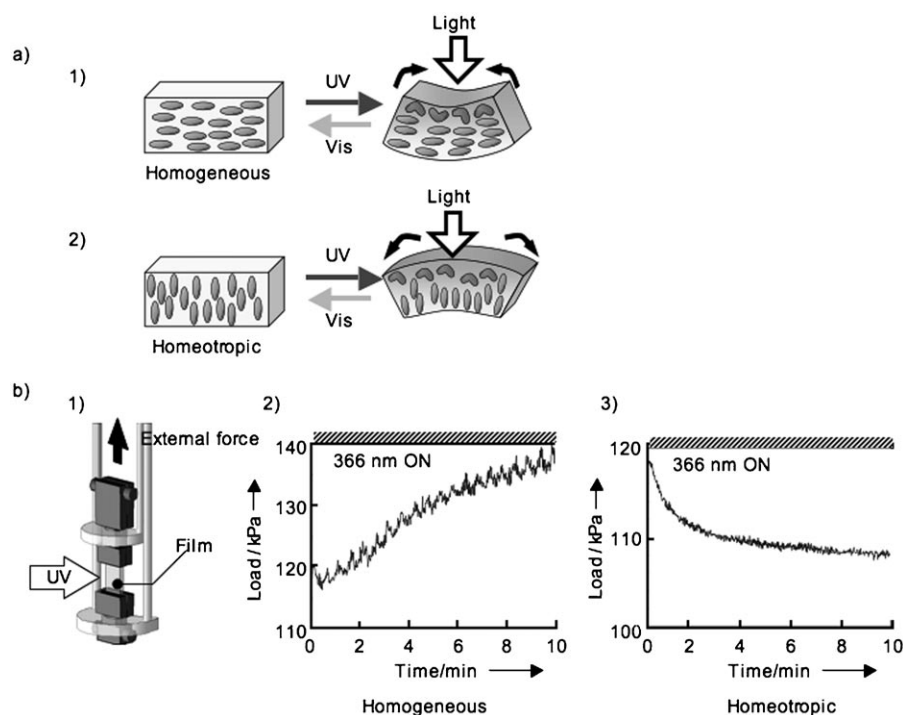


Figure 4. Schematic illustration of the bending mechanism in the homogeneous and the homeotropic films (a) and force generated by photoirradiation (b). Schematic illustration of the experimental setup (1), the force generated upon exposure to UV light at 366 nm (4.8 mW cm^{-2}) in the homogeneous film (2), and the homeotropic film (3). Size of the films: $4.5 \text{ mm} \times 5 \text{ mm} \times 20 \text{ }\mu\text{m}$.

gives rise to *trans*–*cis* isomerization and alignment change of the azobenzene mesogens in LCEs. In the homogeneous films, as the azobenzene mesogens are aligned parallel to the rubbing direction, an anisotropic contraction is generated along this direction upon UV-light irradiation (Figure 4a(1)). On the other hand, the alignment direction of the azobenzene mesogens in the homeotropic films is perpendicular to the film surface; thus, exposure to UV light induces an isotropic expansion (Figure 4a(2)). In addition, because of the high concentration of the azobenzene moieties in both LCE films and the high extinction coefficient of the azobenzene moieties at the irradiation wavelength, the actinic UV light hardly permeates through either film. As a result, an uneven distribution of anisotropic deformation is generated along the film normal in both films: contraction of the surface layer in the homogenous film while expansion of the surface layer

occurs in the homeotropic film. This change in the mode of deformation leads to the bending behavior in a completely opposite direction.

The influence of temperature and light intensity on the bending behavior was examined by measuring the time taken by both films to bend by 90° . It was observed that the bending was accelerated by increasing the temperature and the light intensity.

To confirm the mechanism of bending in these two films, we measured the mechanical force generated from photoirradiation by thermomechanical analysis. As shown in

Figure 4b(1), a film was first fixed by clamping both ends of the film and heated to 75°C , which is higher than the T_g value of the film. An external force was loaded onto the film to keep the length of the film unchanged. The stretching direction was parallel to the alignment direction for the homogeneous film. Upon irradiation of UV light, the load of the homogeneous film increased from approximately 120 to 140 kPa after photoirradiation for 10 minutes (Figure 4b(2)). On the contrary, the load of the homeotropic film decreased from approximately 120 to 110 kPa after photoirradiation for 10 minutes (Figure 4b(3)). These results clearly indicate that the surface region in the homeotropic film expands, while that in the homogeneous film contracts along the alignment direction. In addition, it was found that the time taken for the homeotropic film to reach the maximum force was faster than that of the homogeneous film, presumably because the absorbance of the homeotropic film is lower than that of the homogeneous film. Thus, the light penetrates the film more

deeply in the homeotropic film than the homogeneous film and the change in alignment of mesogens is induced in a thicker layer in the former than in the latter, which would lead to the observed difference in the photomechanical effect in the two films.

In conclusion, the initial alignment of photoactive mesogens significantly affects the bending behavior of the LCE films: the homogeneous films bent toward the irradiation direction of the actinic UV light, while the homeotropic films bent away from the light source. The change in the photo-induced bending behavior is assumed to arise from the different mode of deformation of the surface layer of the two films. The surface of the homogeneous films contracts and the load on the films increases, while the surface of the homeotropic films expands and the load on the films decreases upon exposure to UV light.

Experimental Section

LC monomer A6AB6 and cross-linker DA6AB were prepared according to a previously reported method.^[23] The LCE films were prepared by in situ photopolymerization of a mixture of A6AB6 and DA6AB (90:10 (mol/mol)) containing 1 mol% of photoinitiator (Ciba Specialty, Irgacure 784). First, the melt of the mixture was injected into a glass cell, which had been treated for homogeneous or homeotropic alignment. The homogeneous cell was coated with polyimide alignment layers that had been rubbed to align LC mesogens, while the homeotropic cell was treated with *n*-octadecyltrimethoxysilane. After the sample was cooled down slowly ($0.5^{\circ}\text{Cmin}^{-1}$) to a polymerization temperature at 88°C (in the N phase), photoirradiation was performed at $>540\text{ nm}$ (547 nm , 3 mWcm^{-2}) with a 500-W high-pressure mercury lamp through glass filters (Toshiba, Y-52 + IRA-25) for 2 h. The LCE films were taken off from the cells after polymerization.

The thermodynamic properties of the monomers and the LCE films were determined by DSC (Seiko I&E, SSC-5200 and DSC220C) at heating and cooling rates of $2^{\circ}\text{Cmin}^{-1}$ for the monomers and $10^{\circ}\text{Cmin}^{-1}$ for the films. At least three scans were performed to check the reproducibility. The films were washed with CHCl_3 to completely remove the starting monomers and dried under reduced pressure. The mesomorphic properties and the phase-transition behavior were examined with a polarizing optical microscope (POM; Olympus, BH-2) equipped with a Mettler hot stage (models FP-90 and FP-82). The polarized UV spectra of the films were measured at room temperature with a UV/Vis absorption spectrometer (Jasco, V-550). Thermomechanical analysis was performed in a stretch mode under an external tension at a constant temperature, using a thermomechanical analyzer (TMA; Simadzu, TMA-60).

Received: October 18, 2005

Published online: January 20, 2006

Keywords: alignment · azobenzene derivatives · elastomers · liquid crystals · surface chemistry

- [1] M. V. Gandhi, B. S. Thompson, *Smart Materials and Structures*, Chapman and Hall, London, **1992**.
- [2] Y. Osada, D. E. E. Derossi, *Polymer Sensors and Actuators*, Springer, Heidelberg, **2000**.
- [3] E. Smela, *Adv. Mater.* **2003**, *15*, 481–494.
- [4] R. Pelrine, R. D. Kornbluh, Q. Pei, J. Joseph, *Science* **2000**, *287*, 836–839.
- [5] G. H. Haertling, *Proc. SPIE-Int. Soc. Opt. Eng.* **1997**, *3040*, 81–92.
- [6] A. D. Johnson, V. Martnov, V. Gupta, *Proc. SPIE-Int. Soc. Opt. Eng.* **2001**, *4557*, 341–351.
- [7] R. D. Kornbluh, R. Pelrine, Q. Pei, R. Heydt, S. Stanford, S. Oh, J. Eckerle, *Proc. SPIE-Int. Soc. Opt. Eng.* **2002**, *4698*, 254–270.
- [8] M. Torres-Lungo, N. A. Pappas, *Macromolecules* **1997**, *30*, 6646–6651.
- [9] Z. Hu, X. Zhang, Y. Li, *Science* **1995**, *269*, 525–527.
- [10] H. Wermter, H. Finkelmann, *Liquid Crystalline Elastomers as Artificial Muscles*, <http://www.e-polymers.org> Report No. 013, **2001**.
- [11] D. L. Thomsen III, P. Keller, J. Naciri, R. Pink, H. Jeon, D. Shenoy, B. R. Ratna, *Macromolecules* **2001**, *34*, 5868–5875.
- [12] J. Naciri, A. Srinivasan, H. Jeon, N. Nikolov, P. Keller, B. R. Ratna, *Macromolecules* **2003**, *36*, 8499–8505.
- [13] A. Lendlein, J. Jiang, O. Jüngerand, R. Langer, *Nature* **2005**, *434*, 879–882.
- [14] S. V. Ahir, E. M. Terentjev, *Nat. Mater.* **2005**, *4*, 491–495.
- [15] M. Warner, E. M. Terentjev, *Liquid Crystal Elastomers*, Oxford University Press, Oxford, UK, **2003**.
- [16] P.-G. de Gennes, M. Hebert, R. Kant, *Macromol. Symp.* **1997**, *113*, 39–49.
- [17] P. Xie, R. Zhang, *J. Mater. Chem.* **2005**, *15*, 2529–2550.
- [18] H. Finkelmann, E. Nishikawa, G. G. Pereira, M. Warner, *Phys. Rev. Lett.* **2001**, *87*, 015501.
- [19] M. Camacho-Lopez, H. Finkelmann, P. Palfy-Muhoray, M. Shelley, *Nat. Mater.* **2003**, *2*, 307–310.
- [20] M.-H. Li, P. Keller, B. Li, X. Wang, M. Brunet, *Adv. Mater.* **2003**, *15*, 569–572.
- [21] T. Ikeda, M. Nakano, Y. Yu, O. Tsutsumi, A. Kanazawa, *Adv. Mater.* **2003**, *15*, 201–205.
- [22] Y. Yu, M. Nakano, T. Ikeda, *Nature* **2003**, *425*, 145.
- [23] D. Caretti, A. S. Angeloni, C. Carlini, M. Laus, E. Chiellini, G. Galli, A. Altomare, R. Solaro, *Liq. Cryst.* **1989**, *4*, 513–527.